Competition between Spin Echo and Spin Self-Rephasing in a Trapped Atom Interferometer

C. Solaro,[1] A. Bonnin,[1] F. Combes,[2] M. Lopez,[1] X. Alauze,[1] J.-N. Fuchs,[2,3] F. Piéchon,[2] and F. Pereira Dos Santos[1,*]
[1]SYRTE, Observatoire de Paris, PSL Research University, CNRS, Sorbonne Universités, UPMC Université Paris 06, LNE, 61 Avenue de l'Observatoire, 75014 Paris, France
[2]Laboratoire de Physique des Solides, CNRS UMR 8502, Université Paris-Sud, Université Paris-Saclay, F-91405 Orsay Cedex, France
[3]Laboratoire de Physique Théorique de la Matière Condensée, CNRS UMR 7600, Université Pierre et Marie Curie, 4 place Jussieu, 75252 Paris Cedex 05, France
(Received 31 May 2016; published 14 October 2016)

We perform Ramsey interferometry on an ultracold ^{87}Rb ensemble confined in an optical dipole trap. We use a π pulse set at the middle of the interferometer to restore the coherence of the spin ensemble by canceling out phase inhomogeneities and creating a spin echo in the contrast. However, for high atomic densities, we observe the opposite behavior: the π pulse accelerates the dephasing of the spin ensemble leading to a faster contrast decay of the interferometer. We understand this phenomenon as a competition between the spin-echo technique and an exchange-interaction driven spin self-rephasing mechanism based on the identical spin rotation effect. Our experimental data are well reproduced by a numerical model.

DOI: 10.1103/PhysRevLett.117.163003

A long coherence time is crucial for the coherent manipulation of quantum systems. In quantum information, high-precision spectroscopy as well as in atom interferometry, preventing pure quantum states from decaying into a statistical mixture is challenging. In particular, when manipulating trapped ensembles, particles experience different trapping potentials and their spins precess at different rates creating a deleterious dephasing of coherences. Several techniques have been developed to overcome this limitation and to extend the coherence of the spin ensemble. The use of a magic wavelength for optically trapped atomic clouds [1,2], the addition of a compensating field [3], or the mutual compensation scheme in magnetically trapped Rb ensembles [4] have been demonstrated. All such techniques, however, only reduce the dephasing that is slowed down but never canceled.

A widespread technique that cancels out inhomogeneous dephasing is to create a spin echo via a π pulse as originally thought of for NMR spectroscopy [5] and later on extended to cold gases [6]. The spin-echo technique reverses the inhomogeneous dephasing of a spin ensemble, which significantly increases the coherence time of the quantum system. Especially, inertial atomic sensors highly benefit from spin-echo techniques as, for symmetric interferometers, it cancels out unwanted clock effects [7], enabling unprecedented high sensitivities on the measurement of inertial forces [8–13]. In such configurations, however, dephasing sources originating from atom transverse motion [14,15] can only be tackled by cooling the particles to lower temperatures, suggesting the use of dense ultracold gases. Yet, in such a regime, collisional processes can also lead to inhomogeneous broadening and decoherence of the spin ensemble [16]. The spin-echo technique can in principle just as well cancel out mean-field shift inhomogeneities which is expected to restore the coherence of a spin ensemble at low temperatures.

However, using Ramsey interferometry and the spin-echo technique on an ultracold ^{87}Rb ensemble confined in an optical dipole trap, we observe the opposite behavior: applying a π pulse in the middle of the Ramsey sequence increases spin dephasing leading to a faster loss of coherence of the spin ensemble. This unexpected phenomenon results from the interplay between the π pulse and a collective spin self-rephasing (SSR) mechanism [17] due to the cumulative effect of the identical spin rotation effect (ISRE) in a trapped collisionless gas. Originating from atomic interactions and indistinguishability, ISRE is responsible for the exchange mean field [18] and is characterized by the exchange rate $\omega_{\mathrm{ex}} = 4\pi\hbar a_{12}\bar{n}/m$, where a_{12} is the relevant scattering length [19], $\bar{n}$ the mean atomic density, and m the atomic mass. In this Letter, we investigate the interplay between the spin-echo technique and SSR, two different rephasing mechanisms that, surprisingly, do not collaborate.

Experimental setup.—In our system, we manipulate laser-cooled ultracold ^{87}Rb atoms trapped in a 3D optical dipole trap red-detuned far from resonance ($\lambda = 1070$ nm). The trap consists of two intersecting beams of 30 and 176 μm waists with maximum powers of 6 and 45 W, respectively. After loading the trap from a magneto-optical trap, we perform 2 s evaporative cooling to reach a cloud temperature of $T \sim 500$ nK with trap frequencies $\{\omega_1, \omega_2, \omega_3\} = 2\pi \times \{27, 279, 269\}$ Hz. With $\bar{n}$ in the range of 10^{12} at/cm^3, we explore the nondegenerate and collisionless (Knudsen) regime where the trap frequencies are much larger than the rate γ_c of lateral collisions. These

collisions are velocity changing elastic collisions, also known to be responsible for collisional narrowing [20]. The rate γ_c is given by $\sim 4\pi a^2 v_T \bar{n}$, where a is the scattering length [21] and $v_T = \sqrt{k_B T/m}$ the thermal velocity of the atoms. $\gamma_c \sim 2.4\bar{n}$ s^{-1} with $\bar{n}$ in 10^{12} at/cm^3 which, in our range of densities, remains lower than 5 s^{-1}. In order to maximize the contrast of our interferometers, while preserving highest atomic densities, the atoms are carefully polarized into the state $|5s^2S_{1/2}, F = 1, m_F = 0\rangle$ to avoid spin relaxation [22] and to minimize their sensitivity to parasitic magnetic fields. During the early stage of evaporation, after switching on our quantification axis, a σ-polarized resonant pulse on the $|5s^2S_{1/2}, F = 1\rangle$ to $|5s^2P_{3/2}, F' = 0\rangle$ transition pumps 70% of the atoms into the dark state $|F = 1, m_F = 0\rangle$. A combination of microwave and optical pulses is then used after the evaporation to purify the atomic sample leading to a highly polarized spin ensemble where $98 \pm 1\%$ of the atoms are in the $|F = 1, m_F = 0\rangle$ state. After this preparation sequence, we use resonant microwave field on the $|F = 1, m_F = 0\rangle$ to $|F = 2, m_F = 0\rangle$ transition and perform Ramsey interferometry. We can implement a standard Ramsey interferometer $(\pi/2 - T_R - \pi/2)$ or add a π pulse in the interferometric sequence $(\pi/2 - t_\pi - \pi - t_2 - \pi/2)$ with $T_R = t_\pi + t_2$. In particular, we can realize a symmetric Ramsey interferometer when $t_2 = t_\pi$. After the interferometer, the atoms are released from the trap and the populations in the two hyperfine states are measured. This state selective detection is based on fluorescence in horizontal light sheets at the bottom of the vacuum chamber [23]. Since this detection system does not resolve the different m_F states, $|F = 2, m_F = \pm 1\rangle$ states that are created during the interferometer sequence by spin relaxation contribute as a background, which reduces the contrast by about 15% for $T_R = 1$ s and $\bar{n} = 2 \times 10^{12}$ at/cm^3.

First experiment.—To illustrate the effect of the spin-echo technique and SSR onto the coherence of the spin ensemble, we display in Fig. 1 measurements of the Ramsey contrast with and without a π pulse for different atomic densities $\bar{n}$. To vary $\bar{n}$, we vary the number of atoms by changing the magneto-optical trap loading time, accessing densities from 0.3 to 2.5×10^{12} at/cm^3 which modulate $\omega_{ex}/2\pi = 7.5\bar{n}$ Hz with $\bar{n}$ in 10^{12} at/cm^3. The cloud temperature was verified to remain constant within 15%. In this regime, inhomogeneous dephasing originates both from differential light shift induced by the trapping lasers and from mean-field interactions, and has for characteristic inhomogeneity $\Delta_0/2\pi = k_B T/2h \times \delta\alpha/\alpha + 2\sqrt{2}\hbar(a_{11} - a_{22})\bar{n}/m$ using the same definition of Δ_0 as in [17,24]. Here, $\delta\alpha$ and α are the differential and the total light shift per intensity. With $\delta\alpha/\alpha = 5.93 \times 10^{-5}$ and a_{11}, a_{22} the relevant scattering lengths [19] we have $\Delta_0/2\pi \approx 0.3 + 0.7\bar{n}$ Hz with $\bar{n}$ in 10^{12} at/cm^3. The Ramsey time is $T_R = 2t_\pi = 0.4$ s and the Ramsey fringe contrast is deduced by scanning the phase of the exciting field. Without any π pulse, the contrast increases with the atomic density (Fig. 1, black dots), revealing the efficiency of the SSR mechanism. Applying a π pulse is expected to help with canceling out the inhomogeneous broadening, thus leading to a much higher contrast. For densities between 0.3 and 0.75×10^{12} at/cm^3 the π pulse indeed increases the contrast with respect to a standard Ramsey interferometer, but its efficiency is diminished as the density increases (Fig. 1, red squares). In fact, for higher densities the π pulse actually accelerates the dephasing, but in a nonmonotonic manner so that the contrast reaches a minimum at an intermediate density 1×10^{12} at/cm^3 and then substantially recovers at highest densities. This behavior traduces an unexpected competition between the individual spin echo and the collective SSR mechanisms.

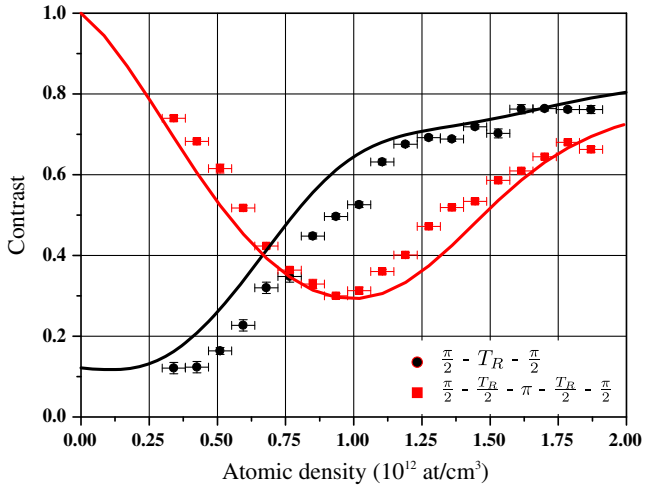

FIG. 1. First experiment: Ramsey fringe contrast as a function of the mean atomic density $\bar{n}$ at a fixed Ramsey time $T_R = 0.4$ s. Red squares and black dots correspond to a Ramsey sequence with and without applying a π pulse at $t_\pi = T_R/2$, respectively. Lines correspond to our simulation results [25]. Black line and dots: the contrast increases with the atomic density which is characteristic of the spin self-rephasing mechanism [17]. Red dashed line and squares: the π pulse is expected to help with canceling out the inhomogeneous broadening leading to a much higher contrast. Surprisingly, for densities larger than 0.75×10^{12} at/cm^3, the π pulse leads to a lower contrast which reaches a minimum at an intermediate density 1×10^{12} at/cm^3. This nonmonotonic behavior suggests a competition between spin echo and spin self-rephasing mechanisms.

Two macrospins model.—SSR was first observed in a magnetically trapped ^{87}Rb ensemble [17] and subsequently employed in an optical trap [24] to extend the coherence time of a spin ensemble. This noteworthy collective mechanism extends the coherence time up to several seconds and leads to revivals of the contrast at periods of the ISRE: $T_{ex} = 2\pi/\omega_{ex}$. Following the two macrospins model of [26], we divide the atomic population into two groups of equal size, each characterized by a macrospin and

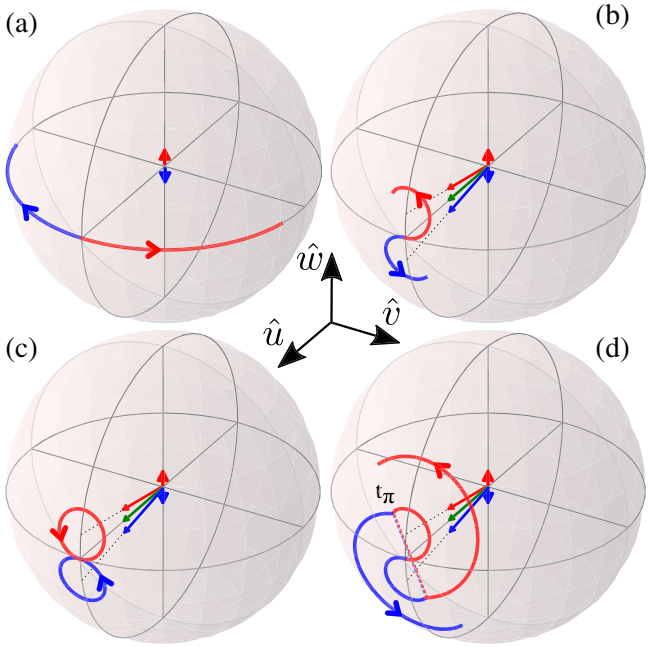

FIG. 2. The atomic population is divided into two equal classes of hot (red) and cold (blue) atoms that are represented by their macrospins trajectories on the Bloch sphere. (a) Inhomogeneous dephasing acts as a torque pointing in the $\hat{\boldsymbol{w}}$ direction that is of opposite sign for the two classes of atoms (red and blue short arrows). (b) With the ISRE, the effective magnetic field seen by the atoms is the sum of the inhomogeneity and the exchange mean field proportional to the total spin (green arrow). As a consequence, the hot (cold) macrospin precesses around the red (blue) long arrow, so that if no π pulse is applied they rephase at time T_{ex}: this is the SSR (c). If one applies a π pulse when the two macrospins are out of the equatorial plane (u, v), the rephasing is degraded (d).

represent them by their trajectory on the Bloch sphere [17,27]. The fast (slow) macrospin corresponds to the hot (cold) atoms which occupy higher (lower) transverse states of the 3D harmonic oscillator. For the sake of simplicity, we consider the dynamics in the rotating frame where the total spin always points in the $\hat{\boldsymbol{u}}$ direction of the Bloch sphere, and the π pulses are rotations of π around this axis. Without the ISRE, the effective magnetic field seen by the macrospins only consists in the inhomogeneity which points along $\hat{\boldsymbol{w}}$ and in opposite directions for the two macrospins. Hence, the fast macrospin rotates towards the right while the slow macrospin rotates towards the left [Fig. 2(a)]. Applying a π pulse at time t_π would swap the two macrospins, so that at time 2 t_π the macrospins would resynchronize leading to a spin echo (not shown). With the ISRE, the effective magnetic field is now the sum of the inhomogeneity and the exchange mean field which is proportional to the total spin. As a consequence, the fast macrospin rotates around this effective magnetic field displayed as the long red arrow in Fig. 2(b), staying in the upper hemisphere of the Bloch sphere, while the slow macrospin evolves in the lower hemisphere. If no π pulse is applied, the macrospins reach the equatorial plane again in their initial direction $\hat{\boldsymbol{u}}$ at the exchange period: the synchronization is perfect [Fig. 2(c)]. However, if a π pulse is applied, swapping the two macrospins positions, their trajectories are not confined to the upper (lower) hemisphere anymore [Fig. 2(d)], so that when they reach the equatorial plane again, they are not aligned: synchronization still occurs but is not perfect anymore. The effect of the π pulse on SSR depends on the ratio between t_π and T_{ex}: when the macrospins are back in the equatorial plane the π pulse has no effect ($t_\pi = pT_{\mathrm{ex}}$ with $p \in \mathbb{N}$), while the effect is worst when the macrospins are maximally out of the equatorial plane [$t_\pi = (p + \frac{1}{2})T_{\mathrm{ex}}$].

Second experiment.—To further investigate the competition, we performed standard and symmetric Ramsey interferometers scanning both the phase and the Ramsey time T_R from 0 to 900 ms. We extract the fringe contrast as a function of time for different atomic densities $\bar{n} = \{0.4, 0.9, 1.7, 2\} \times 10^{12}$ at/cm^3 (Fig. 3). Black circles correspond to standard Ramsey interferometers and are similar to the ones in [17], whereas the red triangles correspond to symmetric Ramsey interferometers ($t_2 = t_\pi = T_R/2$). For the lowest density, inhomogeneous broadening results in a $1/e$ dephasing time of $T_2^\star \approx 0.2$ s corresponding to an inhomogeneity of $\Delta_0 \approx 1/T_2^\star \approx 2\pi \times 0.8$ Hz using the same notations as [28], and agrees within

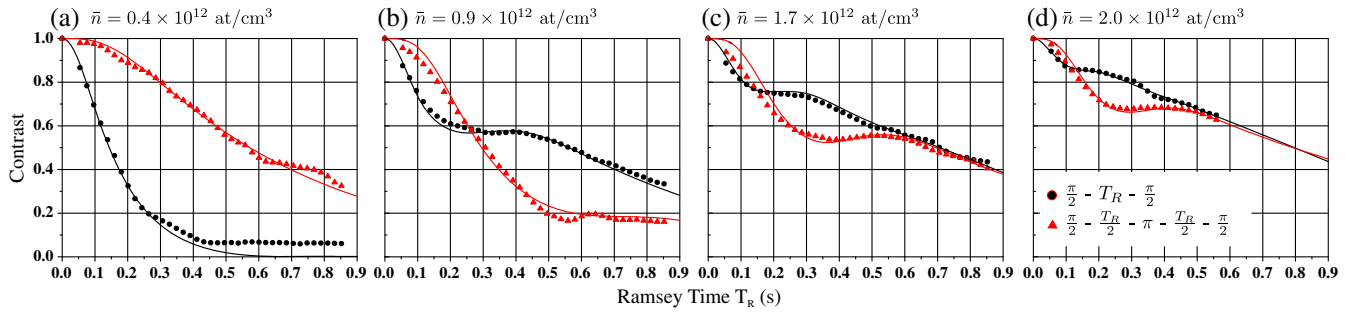

FIG. 3. Second experiment: Ramsey contrast versus Ramsey time T_R for standard Ramsey interferometers (black dots) and symmetric Ramsey interferometers with $t_\pi = T_R/2$ (red triangles). The mean density increasing from (a) to (d) is $\{0.4, 0.9, 1.7, 2.0\} \times 10^{12}$ at/cm^3. Lines correspond to numerical simulations. For details regarding our model and the values of fit constants, see [25].

15% of our estimated inhomogeneity. In this regime we verify that the spin-echo technique is very efficient resulting in a $1/e$ coherence time of $T_2' = 0.8$ s [Fig. 3(a)]. For the highest density, one observes a revival of the standard Ramsey interferometer's contrast at 0.25 s that also corresponds to a local minimum of the symmetric one [Fig. 3(d)]. Such a behavior is what one would expect from the two macrospins model described above. For the standard Ramsey interferometer the spins are fully resynchronized at the exchange period $T_{\rm ex}$ resulting in a revival of the Ramsey contrast at $T_R = 0.25$ s. For the symmetric Ramsey interferometer, for the same Ramsey time, the atoms were swapped by a π pulse at $t_\pi = T_R/2 = 0.125$ s (i.e., at half the exchange period), resulting in an acceleration of the dephasing and the lowest contrast of the interferometer. We observe that same phenomenon for different atomic densities $\bar{n} = \{2, 1.7, 0.9\} \times 10^{12}$ at/cm^3 at different Ramsey time $T_0 \approx \{0.25, 0.32, 0.5\}$ s with about the same scaling $\bar{n}T_0 \approx$ cst. Notice that no such other modulation is clearly observed at multiples $p \neq 1$ of the exchange period as it is expected from our simple model. This can be explained by our relatively high rate of lateral collisions γ_c that perturb SSR, resulting in a damping of the contrast revivals.

Third experiment.—To further understand the spin dynamics and test our numerical model [25], we measured the evolution of the contrast after a fixed π pulse at $t_\pi = 0.125$ s, for three different atomic densities $\bar{n} = \{0.4, 1.1, 2.5\} \times 10^{12}$ at/cm^3 (Fig. 4). We scan the Ramsey time T_R between 0 and 900 ms (with t_2 not necessarily equal to t_π) in order to observe the formation of a spin echo. For the lowest density, we observe a net revival of the contrast at $T_R = 2t_\pi = 0.25$ s. As it is expected when exchange interactions and thus SSR are negligible, the π pulse reverses the inhomogeneous dephasing and leads to a spin echo. For $\bar{n} = 1.1 \times 10^{12}$ at/cm^3, a smaller echo occurs at a time $T_R \approx 0.18$ s $< 2t_\pi$. This behavior is well reproduced by our model and is a consequence of SSR which tends to faster resynchronize the spins after the π pulse. Increasing further the density, one cannot see any echo since for such densities the π pulse is now mostly a perturbation of SSR. But, for Ramsey times $T_R > 2t_\pi$, SSR (re)occurs at time $T_R \approx t_\pi + T_{\rm ex}$ resulting in a net revival of the contrast at ≈ 0.4 s. Note that the same behavior is observed for the intermediate atomic density at $T_R \approx 0.6$ s. It can also be reproduced by the simulation, but with other parameters (in particular, a larger exchange rate), and at the expense of a poorer agreement at short Ramsey times. This behavior remains to be explained.

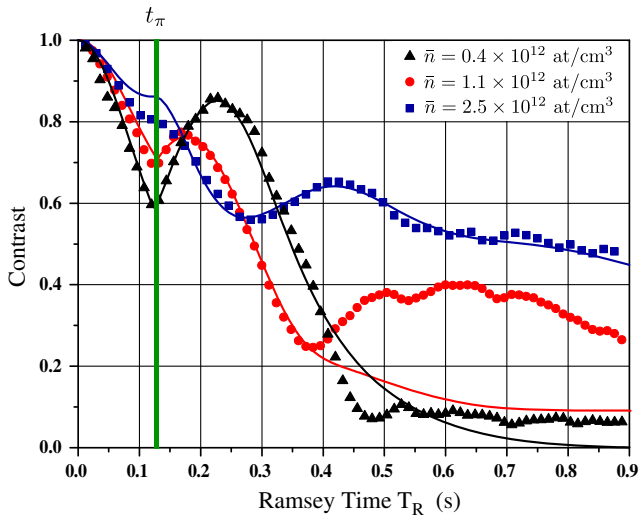

FIG. 4. Third experiment: Ramsey contrast versus Ramsey time T_R with a fixed π pulse at $t_\pi = 125$ ms (green vertical line). Black triangles, red dots, and blue squares correspond to the experimental data for different atomic densities. Lines correspond to numerical simulations [25].

In summary, we have investigated both experimentally and theoretically the interplay between the spin-echo technique and the spin self-rephasing mechanism in a trapped atom interferometer. In particular, we show that the complex spin dynamics resulting from the competition between these two effects leads to nontrivial evolution of the coherence of the atomic ensemble. We propose a simple two macrospins model to give a qualitative insight into this dynamics. We also find a quantitative agreement between our measurements and the results of a numerical simulation.

Spin echoes have been used in a recent work [29] to observe the effect of the ISRE onto the spin diffusion coefficient of a unitary degenerate gas, allowing for the determination of the Leggett-Rice parameter [30]. Notice that in such a study, by contrast to our situation, SSR is absent as the gas is in the hydrodynamic rather than collisionless regime.

Our results illustrate the crucial role played by atomic interactions, in some cases deleterious, in others beneficial, in the dynamics of quantum sensors based on ultracold atoms. In particular, the spin dynamics and coherence of atom interferometers depend on the geometry of the sensor, through the details of the pulse sequence one uses. Whereas the spin-echo technique is not used in standard Ramsey microwave interferometry for clock spectroscopy and frequency measurements, it is widely used in other interferometer configurations as, for example, for the measurement of inertial forces, where π pulses are used to cancel out all clocks effects. However, in such interferometers, the two partial wave packets associated to the two internal states do not overlap perfectly and ISRE is expected to be weaker. The dependance of SSR with this overlap can be studied in an interferometer using atoms trapped in a lattice, such as [31]. Another interesting perspective would be to investigate if a modified π pulse (e.g., a *mirror* pulse [25]) would allow producing better spin echoes in the presence of ISRE. Similar issues are currently being studied in the context of many-body interacting quantum systems [32].

We thank Peter Rosenbusch, Wilfried Maineult, and Kurt Gibble for useful discussions. We also acknowledge financial support by the IDEX PSL (ANR-10-IDEX-0001-02 PSL) and ANR (ANR-13-BS04-0003-01). A. B. thanks the Labex First-TF for financial support.

*franck.pereira@obspm.fr

[1] H. Katori, M. Takamoto, V. G. Palchikov, and V. D. Ovsiannikov, Phys. Rev. Lett. **91**, 173005 (2003).
[2] H. Katori, K. Hashiguchi, E. Y. Ilinova, and V. D. Ovsiannikov, Phys. Rev. Lett. **103**, 153004 (2009).
[3] A. Kaplan, M. F. Andersen, and N. Davidson, Phys. Rev. A **66**, 045401 (2002).
[4] H. J. Lewandowski, D. M. Harber, D. L. Whitaker, and E. A. Cornell, Phys. Rev. Lett. **88**, 070403 (2002).
[5] E. L. Hahn, Phys. Rev. **80**, 580 (1950).
[6] M. F. Andersen, A. Kaplan, and N. Davidson, Phys. Rev. Lett. **90**, 023001 (2003).
[7] M. Kasevich and S. Chu, Phys. Rev. Lett. **67**, 181 (1991).
[8] I. Dutta, D. Savoie, B. Fang, B. Venon, C. L. Garrido Alzar, R. Geiger, and A. Landragin, Phys. Rev. Lett. **116**, 183003 (2016).
[9] C. Freier, M. Hauth, V. Schkolnik, B. Leykauf, M. Schilling, H. Wziontek, H.-G. Scherneck, J. Müller, and A. Peters, J. Phys. Conf. Ser. **723** 012050 (2016).
[10] P. Gillot, O. Francis, A. Landragin, F. Pereira dos Santos, and S. Merlet, Metrologia **51**, L15 (2014).
[11] Z.-K. Hu, B.-L. Sun, X.-C. Duan, M.-K. Zhou, L.-L. Chen, S. Zhan, Q.-Z. Zhang, and J. Luo, Phys. Rev. A **88**, 043610 (2013).
[12] F. Sorrentino, Q. Bodart, L. Cacciapuoti, Y.-H. Lien, M. Prevedelli, G. Rosi, L. Salvi, and G. M. Tino, Phys. Rev. A **89**, 023607 (2014).
[13] G. W. Biedermann, X. Wu, L. Deslauriers, S. Roy, C. Mahadeswaraswamy, and M. A. Kasevich, Phys. Rev. A **91**, 033629 (2015).
[14] A. Clairon, A. Landragin, S. Merlet, and F. Pereira dos Santos, New J. Phys. **13**, 065025 (2011).
[15] A. Hilico, C. Solaro, M.-K. Zhou, M. Lopez, and F. Pereira dos Santos, Phys. Rev. A **91**, 053616 (2015).
[16] D. M. Harber, H. J. Lewandowski, J. M. McGuirk, and E. A. Cornell, Phys. Rev. A **66**, 053616 (2002).
[17] C. Deutsch, F. Ramirez-Martinez, C. Lacroûte, F. Reinhard, T. Schneider, J. N. Fuchs, F. Piéchon, F. Laloë, J. Reichel, and P. Rosenbusch, Phys. Rev. Lett. **105**, 020401 (2010).
[18] C. Lhuillier and F. Laloë, J. Phys. (Paris) **43**, 197 (1982).
[19] We use $a_{11} = 101.284a_0$, $a_{22} = 94.946a_0$, and $a_{12} = 99.427a_0$ as calculated by C. Williams and found in Y. R. P. Sortais, Ph.D. thesis, Université Pierre et Marie Curie–Paris VI, 2001.
[20] Y. Sagi, I. Almog, and N. Davidson, Phys. Rev. Lett. **105**, 093001 (2010).
[21] This expression for γ_c assumes $a_{11} \approx a_{22} \approx a_{12} \approx 100a_0 \approx a$ as for ^{87}Rb.
[22] A. Widera, F. Gerbier, S. Fölling, T. Gericke, O. Mandel, and I. Bloch, Phys. Rev. Lett. **95**, 190405 (2005).
[23] A. Clairon, P. Laurent, G. Santarelli, S. Ghezali, S. Lea, and M. Bahoura, IEEE Trans. Instrum. Meas. **44**, 128 (1995).
[24] G. K. Büning, J. Will, W. Ertmer, E. Rasel, J. Arlt, C. Klempt, F. Ramirez-Martinez, F. Piéchon, and P. Rosenbusch, Phys. Rev. Lett. **106**, 240801 (2011).
[25] See Supplemental Material at http://link.aps.org/supplemental/10.1103/PhysRevLett.117.163003 for details regarding our numerical model.
[26] F. Piéchon, J. N. Fuchs, and F. Laloë, Phys. Rev. Lett. **102**, 215301 (2009).
[27] K. Gibble, Physics **3**, 55 (2010).
[28] S. Kuhr, W. Alt, D. Schrader, I. Dotsenko, Y. Miroshnychenko, A. Rauschenbeutel, and D. Meschede, Phys. Rev. A **72**, 023406 (2005).
[29] S. Trotzky, S. Beattie, C. Luciuk, S. Smale, A. B. Bardon, T. Enss, E. Taylor, S. Zhang, and J. H. Thywissen, Phys. Rev. Lett. **114**, 015301 (2015).
[30] A. J. Leggett and M. J. Rice, Phys. Rev. Lett. **20**, 586 (1968).
[31] B. Pelle, A. Hilico, G. Tackmann, Q. Beaufils, and F. Pereira dos Santos, Phys. Rev. A **87**, 023601 (2013).
[32] T. Engl, J. D. Urbina, and K. Richter, arXiv:1409.5684v3.